LOCALIZED CORROSION IN AN H_2S / CO_2 ENVIRONMENT

Bruce Brown, David Young, and Srdjan Nešić
Institute for Corrosion and Multiphase Technology,
Department of Chemical and Biomolecular Engineering, Ohio University
342 West State Street, Athens, Ohio 45701

ABSTRACT

Large scale research is underway in an effort to understand the mechanisms that lead to localized corrosion in the presence of H_2S and CO_2. An initial series of flow loop experiments have been conducted over 30 day intervals at 60ºC, 7.7 bar partial pressure CO_2, pH 6.0,1 wt% NaCl, and partial pressures of H_2S from 0.1 mbar to 1.0 mbar with an additional experiment conducted at 1.0 mbar H_2S and 10 wt% NaCl. This large-scale research was conducted in a 1950-liter system constructed with 10 cm I.D. pipelines of Hastelloy C-276. Corrosion monitoring is conducted by weight loss (WL) coupons and electrochemical measurements of linear polarization resistance. Analysis by SEM is enhanced by the use of an Infinite Focus Microscope (IFM) to digitize the corrosion product film morphology and the surface features of the steel after corrosion product film removal. Electron dispersion spectroscopy and x-ray diffraction are used for compositional analysis of the corrosion product film. Localized corrosion was observed at 0.25 mbar H_2S and at 10 mbar H_2S where corrosion product films played a role in the process.

Keywords: Localized corrosion, hydrogen sulfide, carbon dioxide, iron sulfide, iron carbonate, surface analysis, infinite focus microscope, multiphase flow, single-phase flow, saturation.

INTRODUCTION

Current research in the field of CO_2 corrosion is being driven by industrial research demands to define and characterize localized corrosion. The first definition of the focus area for localized attack was provided in 2003[1]. Three areas, graphically shown in Figure 1, provide a simplified explanation of the probability of localized corrosion based upon corrosion product film protectiveness. The "gray zone," as it was termed, is where a partially protective film on the surface of the carbon steel provides the opportunity for anodic and cathodic sites to be developed, thus propagating localized corrosion through galvanic corrosion. Having experimental conditions in the "gray zone" during iron carbonate film formation has been seen to facilitate propagation of localized attack[2] independent of the mechanism of localized corrosion initiation.

The question is whether or not this same argument of an iron carbonate "gray zone" is valid when hydrogen sulfide is present. It has been observed that trace amounts of H_2S retard the initial corrosion rates over the first 4 days of exposure in non-film forming conditions by approximately 80% for the temperature ranges of 20°C to 80°C.[3] The relationship shown in Figure 2 is for three concentrations of H_2S in two different types of systems without iron carbonate corrosion product film. If the environmental conditions promote precipitation of iron carbonate film and the presence of hydrogen sulfide promotes precipitation and/or solid state reaction to form iron sulfide films, can we define which is the dominant corrosion reaction? Can we use this to predict if localized corrosion is expected?

The experimental parameters for this series of tests were chosen to cover a range of saturation values of iron sulfide (mackinawite) and iron carbonate. An attempt was also made to provide an environment where competition of these two types of corrosion product films may be observed in both single phase and multiphase (gas/liquid) flow regimes and could lead to localized corrosion. The experimental test matrix is listed in Table 1 and the environmental factors that have been under investigation as variables in this series of tests are listed in the left hand column of Table 2. Table 2 is arranged with increasing partial pressure of hydrogen sulfide (pH_2S) and increasing sodium chloride concentration (NaCl) from left to right. The calculated values for saturation of iron carbonate $S(FeCO_3)$ or iron sulfide $S(FeS)$ are shown for each test in Table 1, but are characterized in Table 2 as "Under Saturated," "Near Saturation," "Saturated," or a magnitude(s) larger than the other saturation level.

Linear polarization resistance measurements (LPR) have been historically collected for comparison in H_2S / CO_2 environments, but the results are usually dominated by the presence of H_2S where coverage effects and conductive films give irregular results. For this reason, weight loss coupons (WL) have been used to provide a better indication of the corrosion rate and also provide more information associated with the corrosion product film. A review of the corrosion product films developed on the WL coupons under the tested conditions is provided with explanations.

EXPERIMENTAL METHOD

All experiments listed in Table 1 were conducted in a 1950 liter multiphase flow loop with 350 gallons (~1300 liters) of D.I. water with the appropriate amount of reagent grade sodium chloride added to create the brine. The procedure for operation and experimentation with regard to the "Hydrogen Sulfide System" is outlined in a previous study[4,5]. All experimental parameters, such as pH, temperature, partial pressures, and iron concentration, are adjusted and/or measured for stable conditions prior to the insertion of all flush mounted probes. Corrosion monitoring was mainly conducted using electrically isolated weight loss (WL) coupons with linear polarization resistance (LPR) and electrochemical impedance spectroscopy (EIS) measurements conducted with a concentric ring probe.

The internal pipeline conditions were well controlled for all tests. A total pressure of 8 bar with CO_2 as the dominant component gas was used to provide a stable and abundant source of carbonic acid. Changes in pH were only due to changes in iron concentration and, due to the large volume of the H_2S multiphase flow loop, were normally insignificant. The partial pressure of H_2S was adjusted in the following tests since it was the most dilute component in the solution and is also a consumable in the corrosion reaction. Iron concentrations were initially set at the beginning of each experiment and then measured throughout the test. Temperature is maintained in the tank and monitored in both the tank and the flow loop multiphase test section; changes in temperature are less than ± 2°C during each entire test.

Gas and liquid flow rates are controlled by positive displacement progressive cavity pumps which move volumes of liquid or gas/liquid mixtures continually through the system.

Iron concentration was determined by using a calibrated Turner SP870 Spectrophotometer. Since the "Hydrogen Sulfide System" does not have a means to control iron concentration, this parameter was measured "as is." Liquid samples were taken directly into a beaker with a small amount of HCl to lower the pH and keep the iron in solution. Ten milliliters of the solution were mixed with a phenanthroline reagent to produce a change in color directly related to the concentration of iron in solution.

H₂S concentration in the gas phase is measured with a GASTEC model GV-100S piston pump and various detection tubes. A needle valve was used to release gas from the gas phase of the "Hydrogen Sulfide System" into a directional tube where the measurement took place before the gas was vented. The length of color change in the detection tube reagent was measured using calipers to increase the accuracy of the value. Repeatability of this method was found to be ±5%.

The three major factors that determine the saturation value or magnitude of supersaturation for iron carbonate and iron sulfide are the iron ion concentration, $[Fe^{2+}]$, the carbonate ion concentration, $[CO_3^{2-}]$, and the bisulfide concentration, $[HS^-]$. Using species concentrations based on the physicochemical model of CO_2 corrosion of mild steel,[6] the saturation values were calculated. Saturation values for mackinawite, $S(FeS)$, were calculated using the solubility product with temperature (T) in Kelvin.[7] The saturation value for iron carbonate, $S(FeCO_3)$ was calculated using the equation for solubility product[8] with temperature (T) in °C and ionic strength (I) in mol/L.

$$S(FeS) = \frac{[Fe^{2+}][HS^-]}{[H^+]Ksp(FeS)}$$

(EQ. 1)

$$Ksp(FeS) = \frac{2848.779}{T} - 6.347$$

(EQ. 2)

$$S(FeCO_3) = \frac{[Fe^{2+}][CO_3^{2-}]}{Ksp(FeCO_3)}$$

(EQ. 3)

$$\log K_{sp}(FeCO_3) = -59.3498 - 0.041377(T) - \frac{2.1963}{T} + 24.5724[\log(T)]$$
$$+ 2.518(I^{0.5}) - 0.657(I)$$

(EQ. 4)

The iron concentration $[Fe^{2+}]$ is a measured value, while the carbonate ion $[CO_3^{2-}]$ and bisulfide $[HS^-]$ concentrations are calculated using thermodynamics based on the pH ($-\log[H^+]$) and the partial pressures of CO_2 and H₂S in the gas phase, respectively. During these experiments, carbon dioxide was the dominant gas and, therefore, was an easily maintained parameter, so the carbonate concentration was constant. The hydrogen sulfide concentration in the gas phase varied slightly with time and was

adjusted as necessary. The thermodynamic constants and calculations used for iron carbonate and iron sulfide saturation have been previously reported.[5]

General corrosion values were calculated by subtracting the initial coupon weight from the final coupon weight after Clarke solution cleaning[9] of films and dividing by the exposure time. Localized corrosion rate values were determined by cross-section analysis, calibrated metallurgical microscope depth measurements, and in later testing by the use of an infinite focus microscope (IFM).

RESULTS AND DISCUSSION

With the knowledge that partially protective films can lead to localized corrosion, the goal of this research was to provide conditions where the corrosion product film would be formed in competition between iron carbonate and iron sulfide while also documenting the experimental conditions that lead to localized corrosion. Trace amounts of H_2S (0.25 to 10 mbar partial pressures) were used in this series of experiments in order to observe where the effect of hydrogen sulfide on CO_2 corrosion begins. It is understood that trace amounts of H_2S retard corrosion in a non-film forming environment,[3] but the effect of H_2S on CO_2 corrosion in a system where the iron carbonate saturation is not much greater than unity has not been well covered. This is an important aspect of CO_2 corrosion since previous testing has shown that in a system with a partial pressure of CO_2 and fluid conditions where iron carbonate saturation (EQ. 1) is in the range from 1 to 10, localized corrosion has been observed to propagate.[10]

The first three experiments in this series have been documented previously,[5] but are necessary to revisit in order to compare the corrosion product film morphology with the type of corrosion developed in each test condition.

Experiment 1

In line with the goal of development of competitive films, the first experimental conditions were adjusted so the average value for iron sulfide bulk saturation (EQ. 1) was almost equivalent to the value for iron carbonate bulk saturation (EQ. 3); therefore, the surface films should be a mixture of both precipitates. Localized corrosion was observed in this experiment.

The iron concentration diminished during this experiment, from 10 ppm ± 2 ppm in the beginning to 4 ppm ± 0.2 ppm after 30 days, which can be explained by having precipitation kinetics faster than corrosion kinetics. The effect of a trace amount of H_2S on the CO_2 corrosion rate was easily observed by the corrosion rates measured. Integration of the LPR measurements over the 30 day experiment were 0.076 mm/yr in single phase and 0.018 mm/yr in multiphase as compared to 0.072 mm/yr in single phase and 0.058 mm/yr in multiphase for the weight loss coupons. At these conditions *without the presence of H_2S*, measured and predicted values of CO_2 corrosion should be well over 10 mm/yr.

20 days. The film formed on the surface of the weight loss coupons under these conditions proved to be weak and non-protective. The weight loss coupon from multiphase flow, as shown in Figure 3, was removed after 20 days of exposure to system conditions and shows signs of flow induced degradation of the film. A comparison of the damage on the film surface to the damage of the underlying base material of the same coupon shows that flow induced localized corrosion (FILC) did occur. FILC is seen in more cases involving partial pressures of CO_2 and not H_2S. A weight loss coupon exposed for 30 days under these conditions shows significant film deposition and localized corrosion in

the cross section analysis, Figure 4. The film deposition of approximately 75μm in the cross-section also shows pitting corrosion under the uneven film surface of an additional 45μm in depth.

Pitting factor is defined as the maximum penetration rate divided by the general corrosion rate and is shown to be 3.7, or approximately 4, for 10 days exposure in experiment 1.

Figure 4 also provides a comparison between an SEM image and a backscatter SEM image for the same location on the mild steel coupon exposed for 30 days. The corrosion product layer does not have an easily discernable crystal structure, but does seem to have porosity as shown by color changes in the backscatter SEM. Both the SEM image and the backscatter SEM image show active pit growth in three locations after this exposure time. The dark locations in the pit areas of the backscatter SEM are proof of an existing detached film area where corrosion is occurring.

Experiment 2

When the iron carbonate and iron sulfide saturation values were kept below 5 in the second test, no localized corrosion was observed. Weight loss coupon surface analysis shows minimal corrosion product film in the cross section analysis of Figure 5 with film depth of approximately 25 μm. The maximum WL corrosion rate measured over the 30 days experiment was 0.2 mm/yr. Without an observable corrosion product film, the possibility of localized corrosion was considerably minimized.

EIS data was collected for experiment 2 (Figure 7) and seems to show a rapid surface coverage by a mass transfer limiting film within the first 9 hours of exposure due to the extremely high impedance. Film growth stabilized after the first day of exposure to system conditions as the EIS data is similar and repeated up to day 22 when an infinite polarization resistance is seen to the end of the experiment. The assumption of a full coverage of the surface with a thin film that retards the corrosion rate for the remainder of the experiment is in agreement with WL images and corrosion rates.

30 days. The most important piece of information to come from this testing was the composition of the corrosion product film. Electronic Dispersion Spectroscopy (EDS) detected sulfur and iron elements in the film as expected. X-Ray Diffraction (XRD) was used and measurable peaks indicated a crystal structure present in the films. A similar film composition was measured by XRD for three separate coupons and is represented by the peaks of intensity *vs.* Bragg angle (2θ). Analysis was done by comparison to standard XRD spectra. Comparison for iron sulfides shows no correlating peaks for mackinawite, one possibility for marcasite at $2\theta = 51°$, and four matches for pyrrhotite at $2\theta = 31.5°$, $44.0°$, $52.1°$, and $65.0°$. Comparison to iron carbide again only shows one possible match at $2\theta = 44.4°$ (which was seen previous as pyrrhotite), but five of eight major peaks correlated for siderite at $2\theta = 24.9°$, $32.1°$, $42.4°$, $52.9°$, and $61.8°$. The conclusion from XRD results is that pyrrhotite films and iron carbonate (siderite) films were formed on the coupon surface under the recorded conditions, as seen in Figure 6.

Experiment 3

The third experiment associated with iron carbonate and iron sulfide saturation values set the iron sulfide saturation value (EQ. 1) at a magnitude higher than the iron carbonate saturation value (EQ. 3). Cross sectional analysis shows a maximum 150 μm film thickness was measured for a sample exposed for 30 days to these conditions as shown in Figure 8, but there was no localized corrosion observed. Other WL coupons had corrosion rates of 0.33 mm/yr in single phase flow and 0.56 mm/yr for multiphase flow.

EIS data for experiment 3 (Figure 9) shows only slight changes occurred in the surface conditions during the entire experiment with a somewhat constant impedance measurement after 4 days of exposure to system conditions. This constant impedance measurement agrees with the results since these coupons measured the highest corrosion rate for all three experiments. Although a thick film was developed, it was calculated to have a greater than 90% porosity and is thought to be dominated by iron carbonate corrosion product.

25 days. XRD provided a similar comparison of films formed in single phase and multiphase to pyrrhotite and siderite peak locations, but electron dispersion spectroscopy (EDS) provided more information on the thicker developed film. EDS spot analysis of a film developed after the 25 day exposure to system conditions in multiphase flow shows that sulfides in the film reside mainly in the upper layers near the solid/fluid interface. A cross-sectional view of the coupon in Figure 8 shows three layers of film developed on the surface. From the surface of the coupon outward, the first 60 micron layer was analyzed with EDS and found to have 0% Sulfur, 40% Iron, 13% Carbon, and 30% Oxygen. The next 60 micron layer was found to have 0% Sulfur, 45% Iron, 13% Carbon, and 16% Oxygen. The outermost 30 micron layer was found to have 11% Sulfur, 33% Iron, 22% Carbon, and 13% Oxygen. Only the outermost 30 μm film thickness is affected by the bulk concentration of H_2S (aq).

Experiment 4

The fourth experiment was based on a magnitude increase in the partial pressure of H_2S. The partial pressure of 10 mbar H_2S is a magnitude greater than previous testing while the partial pressure of CO_2, temperature, and water chemistry values remain constant. From Table 1, it can be seen that the iron sulfide saturation in experiment 4 is similar to experiment 3 and iron carbonate saturation is similar to experiment 2, but neither of these experiments (2 or 3) developed localized corrosion. Comparison of experiment 1 and experiment 4 parameters show two orders of magnitude increase in the partial pressure of H_2S with only half the ferrous iron concentration and localized corrosion was observed in both cases.

10 days. Only the WL coupon exposed for the first 10 days of the experiment in multiphase flow has shown indications of localized corrosion. The surface of the coupon had circular features in multiple locations of the corrosion product film with some diameters of these features approaching 1.5mm. An SEM backscatter image of one circular feature, Figure 10, shows a uniform film composition, but the cross sectional analysis of a similar area, Figure 11, shows multiple film compositions. EDS spot analysis of the film, Figure 11, shows a higher sulfide content in the overlying surface film than in the corrosion product developed within the area of localized attack. This is thought to be caused only by the surface film acting as a diffusion barrier.

What is obvious from Figure 11 is the failure of the corrosion product film through cracking and spalling. The white circular feature in the upper portion of the pit, Figure 11, is caused by a bubble trapped inside the epoxy of the cross sectional mount. This is of interest because it highlights the fact that the corrosion product film in this area was damaged, but intact enough to hold a pocket of air when the epoxy coating was applied. The initiation of localized corrosion is assumed to begin at locations where diffusion of H_2S through the film finds a discontinuity in the corrosion product film or an inclusion in the structure of the metal surface. Growth of the corrosion product underneath the existing film will lift and damage the film due to internal stresses. Iron sulfide species will be larger than the ferrous iron cations or hydrogen sulfide anions and have a lower state of energy as a precipitate. At this location a higher corrosion rate will occur because of the increased mass transfer of species through the

film damaged area, propagating the localized corrosion. The general corrosion rate for a similarly exposed coupon measured 3 mm/yr, but the penetration rate calculated from the maximum variation in the metal surface on this cross section is 9 mm/yr. With a penetration rate 3 times greater than the general corrosion rate, this is considered to be localized corrosion and a greater penetration rate could be possible since the cross sectional image is not guaranteed to show the deepest location of the pit. Many locations similar to this were observed with pit penetration rates up to 12.5 mm/yr documented (Figure 12).

Experiment 5

For experiment 5, the amount of sodium chloride was increased to 10 wt% in solution, a magnitude greater concentration than in previous tests. By increasing the ionic strength of the solution through addition of such a large amount of NaCl, the saturation value for iron carbonate (EQ. 3 & 4) was reduced to below the saturation point for precipitation.   In experiment 5, localized corrosion was not observed.

30 days. An example of the surface film developed under these conditions is shown in Figure 13. The large deposition of salt on the surface is thought to be from the sample removal process in which isopropyl alcohol is delicately flushed across the surface to remove water and caused the sodium chloride present to immediately precipitate. The cracked surface film is assumed to be from drying the sample in order to complete the surface analysis. The associated electron dispersion spectroscopy (EDS) indicates the surface film is still dominated by iron sulfide even in the presence of a high chloride content solution. Cross sectional analysis in Figure 14 shows corrosion on the surface of the coupon to be of the same magnitude as the measured general corrosion rate. Indications of corrosion initiation observed in cross sectional analysis are of the same magnitude as the general corrosion rate and, therefore, cannot be considered as localized attack.

Experiment 6

In the sixth experiment, the partial pressure of H_2S was increased to 10 mbar or an order of magnitude over the experiment 5 with the same 10 wt% NaCl solution. The calculated iron carbonate saturation value was between 1 and 3 while the iron sulfide saturation value was calculated to be between 100 and 300 (Table 1).

10 days. The first coupon to be removed from the environmental conditions after 10 days exposure in single phase flow seems to show localized corrosion. From the cross sectional view in Figure 15, the deepest measurable location is calculated to be 8 mm/yr for the maximum corrosion rate. Weight loss for a similar coupon provided a 5.6 mm/yr general corrosion rate, so the deepest measurable location on the cross section did not validate that localized corrosion occurred.

Coupon cross sectioning is a good method for observing characteristics of the corrosion product film structure on the coupon surface, but is a destructive method that limits other types of analysis. The first sample removed from the experiment after 10 days was cross sectioned to view the film structure, but to obtain more information from each WL coupon, a newly acquired Infinite Focus Microscope (IFM) was employed to capture the surface morphology of the corrosion product film and of the bare metal surface after Clarke solution cleaning. Comparison of these surface morphologies and weight loss measurements provide a much better total visualization of the localized corrosion that occurred.   It should be noted that the flow direction for all IFM images is from the bottom to the top of each photo.

Figure 16 shows a comparison of a multiphase coupon removed from experiment 6 after 10 day's exposure with and without corrosion product film. With film in place (top), a location in the upper left quadrant of the coupon was selected for depth analysis as shown by the diagonal line in the upper left photo and by the line graph in the upper left. The variation of the film surface is rather extreme as compared to all other coupons with a 1.7 mm peak of "debris" located on the coupon surface. The circular area of missing corrosion product film was not attached when the sample was removed from the system. With the corrosion product film removed by Clarke solution (bottom), the upper left quadrant of the coupon again shows where the most surface corrosion activity occurred. Through Clarke solution cleaning of the surface film, the general corrosion rate was calculated to be 2.7 mm/yr and, through IFM analysis, the maximum depth of attack was measured to be 0.36 mm or 14.1 mm/yr by calculation. This is considered to be localized corrosion with a calculation of pitting factor to be 5.3. By maintaining coupon orientation during analysis, direct comparison of corrosion product film to corrosion observed on the metal surface shows a greater build up of corrosion products in the area with the greatest corrosion rate.

This is evidence that the localized corrosion mechanism under these conditions is a failure of the corrosion product film allowing corrosive species direct access to react with the metal surface. Hydrogen sulfide reacts directly with a metal surface, but the iron sulfide molecule is larger than the iron atom it replaced and the surface film develops internal stress which leads to the failure of the film. Localized corrosion in the presence of hydrogen sulfide is shown by the build up of corrosion product film on this basis.

20 days. Figure 17 shows coupons exposed to system conditions during the last 20 days of the experiment. Notice the minimal amount of film weight loss as compared to the 10 day exposure WL coupon; eight times less. Without the excess of film built up on either single phase or multiphase coupon, the corrosion was generally uniform over the surface of the coupon. By analysis with the IFM, locations of high penetration can be easily detected over the full surface of the coupon and analyzed.

For the single phase coupon, a location of 0.16 mm in depth and about 0.1 mm in diameter was found. This calculates to a maximum pit penetration rate of 2.9 mm/yr or a pitting factor of 4 since the general WL corrosion rate was measured at 0.7 mm/yr. For the multiphase coupon, a location of 0.18 mm in depth and about 3.5 mm in diameter was found. This calculated to a maximum pit penetration rate of 3.3 mm/yr or a pitting factor greater than 9 since the general WL corrosion rate measured at 0.36 mm/yr.

30 days. Figure 18 provides 3 dimensional images of the corrosion product film and the surface of the coupon after film removal. This corrosion coupon was in place for the entire test and shows the same features observed for the coupons removed after 10 days exposure. By comparison of the morphology of the corrosion product film to the morphology of the corroded surface, it is obvious that the areas of more metal loss occur under the peaks of corrosion product film.

Similar to the coupons removed after the first 10 days, coupons remaining in for the entire length of the experiment had more surface deposition. Figure 19 shows the coupon removed from single phase after 30 days. Notice that the two large peaks of surface film deposition are positioned over the locations of pits shown after film removal. The corrosion product film, with peaks up to 2.1 mm in height, was 0.87 grams in weight as removed by Clarke solution cleaning procedures. This is 1.5 times larger than the amount removed from the multiphase coupon. This is easily understood because of the difference in exposure time to allow more growth of the film. However, the orientation of the flush mounted coupons adds more perspective to the origins of the film deposition. The multiphase flow

8

coupon is flush mounted at the 6 o'clock position in order to experience the most impact from slug flow turbulence. The 6 o'clock location could be assumed to allow solids that have precipitated in the section of pipe upstream of the corrosion coupon to travel along the bottom and find a resting place on the corroding surface of the coupon, thus explaining the excess film. The single phase coupon is flush mounted at the 1 o'clock position in the pipeline since the effect of flow in single phase is uniformly distributed 360 degrees around the pipeline ID except for gravitational effects of flowing debris. This location is not favorable to deposition of precipitated solids migrating through the pipeline which deposit through gravitational means. By direct comparison, this is proof that the excess corrosion product film developed in both single phase and multiphase was caused by reaction of the species within the bulk fluid to the X65 material during the first 10 days of the experiment. It also provides evidence that system bulk fluid conditions during the last 20 days of the experiment were stable and did not warrant removal of the already developed corrosion product film.

On the single phase coupon after film removal, Figure 19, a location of 0.67 mm in depth and about 4 mm in diameter was found to have the maximum pit penetration rate of 8.1 mm/yr which equates to a pitting factor of 3.2 in this case since the general WL corrosion rate was calculated as 2.5 mm/yr.

Figure 20 shows the multiphase coupon which still had a 0.52 gram film deposited on the surface after the 30 day exposure. The surface of the coupon without the corrosion product film shows localized corrosion as well. A location of 0.96 mm in depth and about 0.2 mm in diameter has a maximum pit penetration rate of 11.8 mm/yr or a pitting factor of 3.1 when compared to the general corrosion rate of 3.8 mm/yr.

SUMMARY

The most important finding during the first three experiments is the realization that without a surface film failure, there can be no galvanic couple between protective and non-protective areas in the corrosion product film. This galvanic couple, necessary to propagate localized corrosion, has been shown by testing [10] and theory [11]. The calculated values for saturation of iron carbonate and iron sulfide may be indicators of when surface films are likely to occur, but are not directly related to the localized corrosion phenomenon since many factors are used in the calculation and each factor has its own direct relationship to the type of film developed.

The fact that localized corrosion was observed in the current data set provides direction in defining the parameters that lead to localized corrosion with trace amounts of H_2S. At partial pressures of H_2S below 1 mbar, the system with 7.7 bar pCO_2 was dominated by carbonic acid and the observed localized corrosion was seen as flow induced localized corrosion (FILC). Whereas, at 10mbar partial pressure of H_2S, the observed corrosion was always a pitting type corrosion with or without excess surface corrosion product film. Under conditions involving H_2S as the determining factor in corrosion mechanism, pitting type corrosion was observed.

Initiation and propagation of localized corrosion can be explained in cases similar to this by understanding the characteristics of the corrosion product layers. The surface corrosion product film can be considered to have lateral strength as it developed in a sheet across the metal surface in a solid state reaction, but is thin and can fail through brittle fracture more than likely caused by internal film stresses. The underlying corrosion product film can be considered to have less structure as it developed as a

precipitate of the corrosion reaction in the area underneath the surface film. This combination proves to initiate and propagate localized corrosion.

CONCLUSIONS

- Corrosion product films play a role in the process of localized corrosion.
  - ✓ Dissolution of iron carbonate films in the presence of H_2S may allow better corrosion retardation by an increase in iron sulfide film formation.
  - ✓ Iron carbonate films interfere with the ability of trace amounts of H_2S to retard the corrosion rate.
  - ✓ A relationship between the saturation values and the probability of localized corrosion is difficult because of the multiple factors involved in the saturation calculation.

- The mechanisms that lead to localized corrosion in the presence of H_2S and CO_2 can be directly related to the characteristics of the corrosion product film and its process of formation.
  - ✓ Localized corrosion was observed where corrosion product film growth had exceeded that of the surrounding area.
  - ✓ Although an amount of corrosion protection is offered by the FeS film, breakdown of this film leads to localized attack.
  - ✓ When H_2S is present in solution, the saturation value for iron carbonate is not an indicator for determining the probability of localized corrosion, but may provide the link towards understanding the propagation of localized corrosion.

REFERENCES

1. Sun, Y., "Localized CO_2 Corrosion in Horizontal Wet Gas Flow," PhD dissertation, Ohio University, 2003.

2. Han, J., et al, "Electrochemical Investigation of Localized CO_2 Corrosion on Mild Steel". Corrosion/2007, paper No. 07323, (Houston, TX: NACE, 2007).

3. Brown, B., Parakala, S., Nesic, S., "CO_2 Corrosion in the Presence of Trace Amounts of H_2S," NACE Corrosion 2004, paper no. 04736.

4. Brown, B., Schubert, A., "The Design and Development of a Large-Scale Multiphase Flow Loop for the Study of Corrosion in Sour Gas Environments," NACE Corrosion 2002, paper no. 02502.

5. Brown, B., Nesic, S., "CO_2 / H_2S Corrosion Under Scale Forming Conditions," NACE Corrosion 2005, paper no. 05625.

6. Nordsveen, M., Nesic, S., Nyborg, R., Stangeland, A., "A Mechanistic Model for Carbon Dioxide Corrosion of Mild Steel in the Presence of Protective Iron Carbonate Films – Part 1: Theory and Verification," Corrosion, May 2003, vol. 59, no. 5, pp 443 – 456.

7. Benning, L.G., Wilkin, R.T., Barnes, H.L., "Reaction pathwasy in the Fe-S system below 100ºC," Chemical Geology, v. 167, 2000, pp25-51

8. Sun, W., "Kinetics of Iron Carbonate and Iron Sulfide Scale Formation in CO_2/H_2S Corrosion," Dissertation, Doctor of Philosophy (PhD), Ohio University, Chemical Engineering, 2006.

9. ASTM G1-81, "Standard Practice for Preparing, Cleaning, and Evaluating Corrosion Test Specimens," Laboratory Corrosion Tests and Standards, Editors: Haynes, G.S., Baboian, R., pp505-509, section 7.7.2, 1985.

10. Han, J., "Localized CO_2 Corrosion: Artificial pit design and test", CC JIP Advisory Board Meeting, Temecula Creek, CA, March 2006.

11. Han, J., "Localized CO_2 Corrosion Propagation Evaluation Method," CC JIP Advisory Board Meeting, Athens, OH, September 2006.

TABLES

Table 1. Test Matrix

Parameter	Exp. 1	Exp. 2	Exp. 3	Exp. 4	Exp. 5	Exp. 6
Temperature	60ºC					
Total Pressure	8 bar					
pCO_2	7.7 bar					
pH	6.0					
Flow	Vsl = 1 m/s, Vsg = 3 m/s				Vsl = 1 m/s	Vsl = 1 m/s, Vsg = 3 m/s
NaCl	1 wt%				10 wt%	10 wt%
pH_2S (mBar)	0.25	0.1	1.2	10	1	10
Fe++ (ppm)	5 - 8	5 - 9	15 – 19	1 – 4	1 – 3	1 – 3
$S(FeCO_3)$	5 - 10	1 - 3	7 - 10	1 – 3	0.2 - 0.5	1 – 3
S(FeS)	5 - 10	2 - 5	80 - 120	100 – 300	10 - 20	100 – 300
Measurements	LPR, EIS, WL, SEM					
Exposure Time	10, 20, 30 days					

Table 2. Observations of Localized Corrosion *vs*. Parameters of Interest.

pH_2S (mbar)	0.1	0.25	1	1.2	10	10
NaCl (wt%)	1	1	10	1	1	10
$S(FeCO_3)$	Near Saturation	Saturated	Under Saturated	Saturated	Near Saturation	Near Saturation
S(FeS)	Near Saturation	Saturated	10 x $S(FeCO_3)$	10 x $S(FeCO_3)$	100 x $S(FeCO_3)$	100 x $S(FeCO_3)$
General Corrosion (mm/yr)		0.9 to 2.7			0.8 to 2.6	0.3 to 1.5
Localized Corrosion Observed	No	YES	No	No	YES	YES
Pitting Factor	n/a	≈ 4 for 20 & 30 days	n/a	n/a	≈ 4 for 10 days	2 to 5 (10 days) 4 to 9 (20 days) 3 to 5 (30 days)

No film	Partially protective film	Fully protective film
High uniform attack	Low/High uniform attack	Low uniform attack
No localized attack	Localized attack	No localized attack

Figure 1. Definition of focus area for localized attack or localized corrosion, termed the "gray zone." [1]
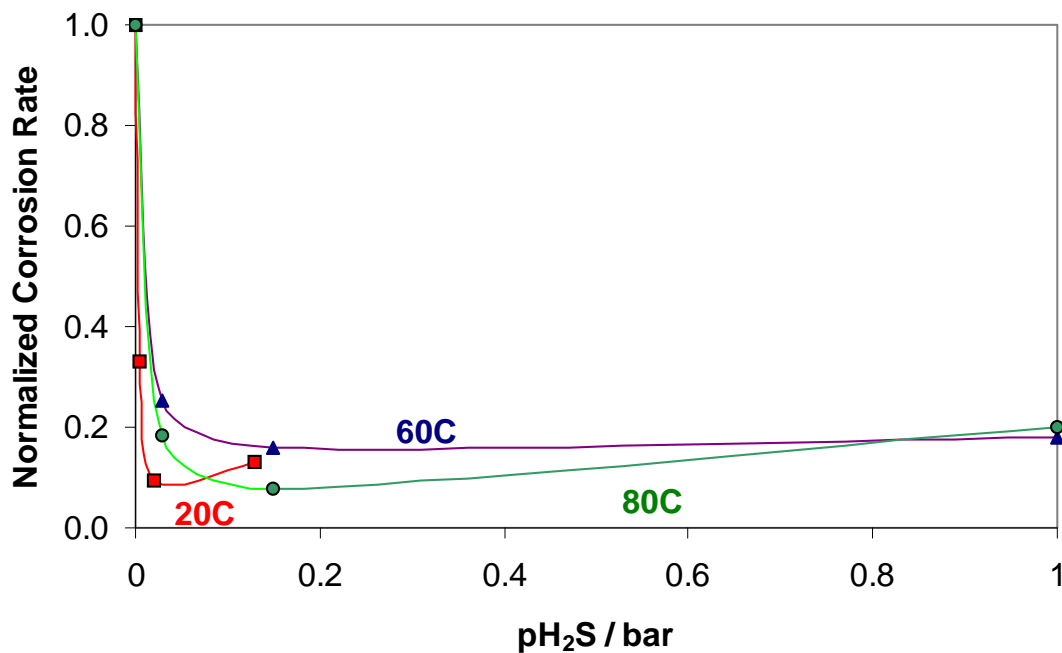
Figure 2. Effect of trace amounts of H_2S on CO_2 corrosion. Normalized LPR corrosion rates measured after 96 hours exposure for different systems at pH4. Testing done in 2L glass cell for 20°C and in Hydrogen Sulfide System for 60°C and 80°C.
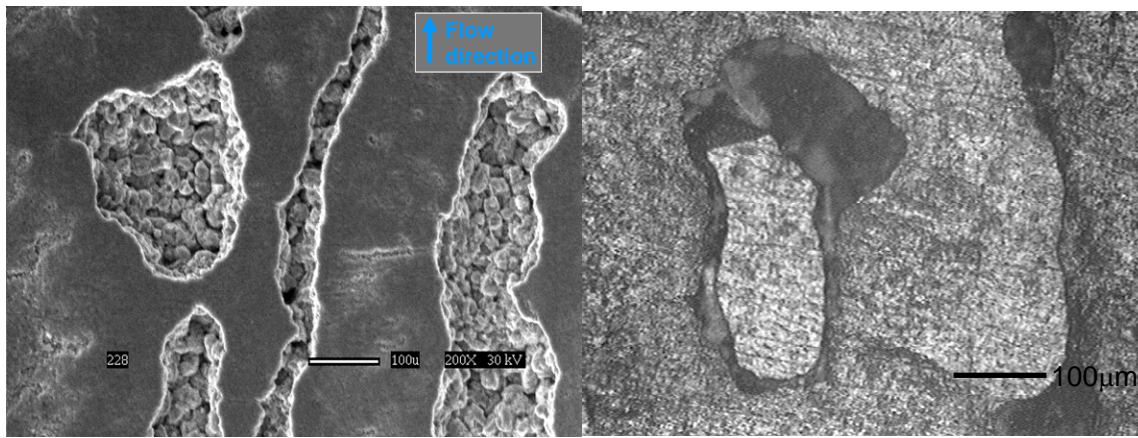
Figure 3. Experiment 1: Observation of flow induced localized corrosion (FILC) in mild steel coupon after 20 days exposure. Morphological relationship shown between film disruption (left) and substrate corrosion (right). (60°C, 7.7 bar pCO_2, 0.25 mbar pH_2S, pH 6, Vsg = 3m/s, Vsl = 1m/s)
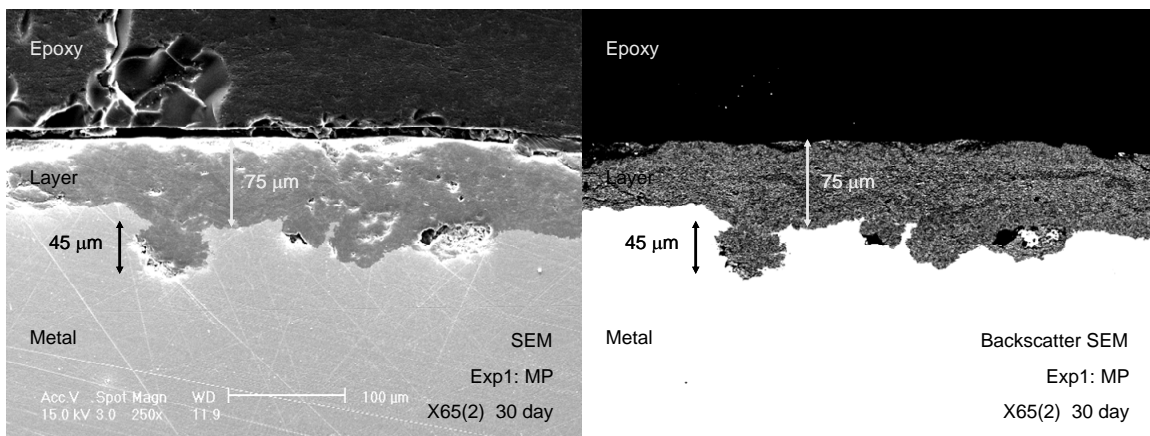
Figure 4. Experiment 1: Cross section of corrosion product film developed after 30 day exposure, SEM (left) and Backscatter SEM (right) images show pit growth under the film. (60°C, 7.7 bar pCO_2, 0.25 mbar p H_2S, pH 6, Vsg = 3m/s, Vsl = 1m/s) Localized Corrosion by max depth: 3.3 mm/yr; General Corrosion by wt loss: 0.89 mm/yr; Pitting Factor: 3.7.
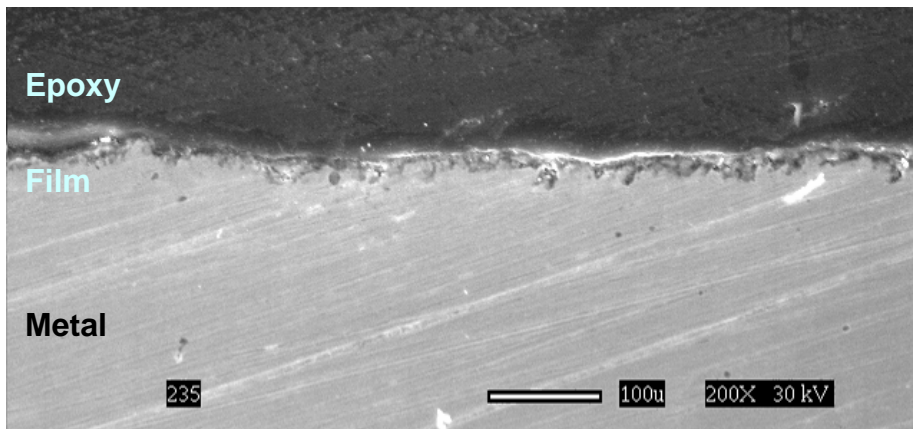
Figure 5. Experiment 2: C1018 MP 30 day exposure, 15 to 30 μm film thickness. (60°C, 0.77 MPa CO_2, pH 6, $pH_2S = 0.10$ mbar, 1wt% NaCl).
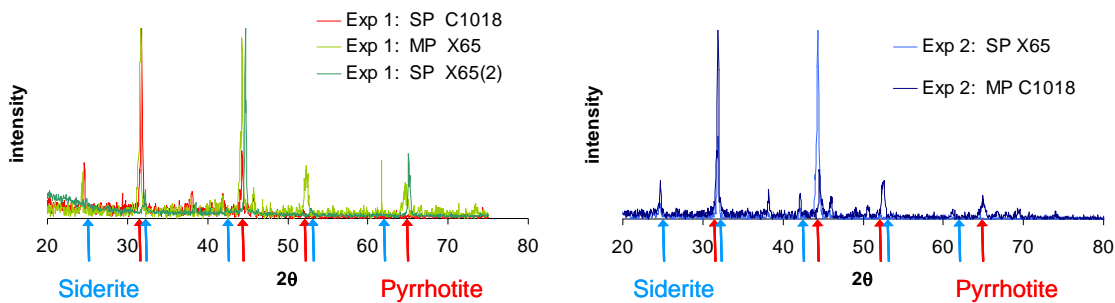
Figure 6. Experiment 1 and 2: XRD comparison from previous designation of siderite and pyrrhotite. Peaks considered "matches" are marked with arrows.
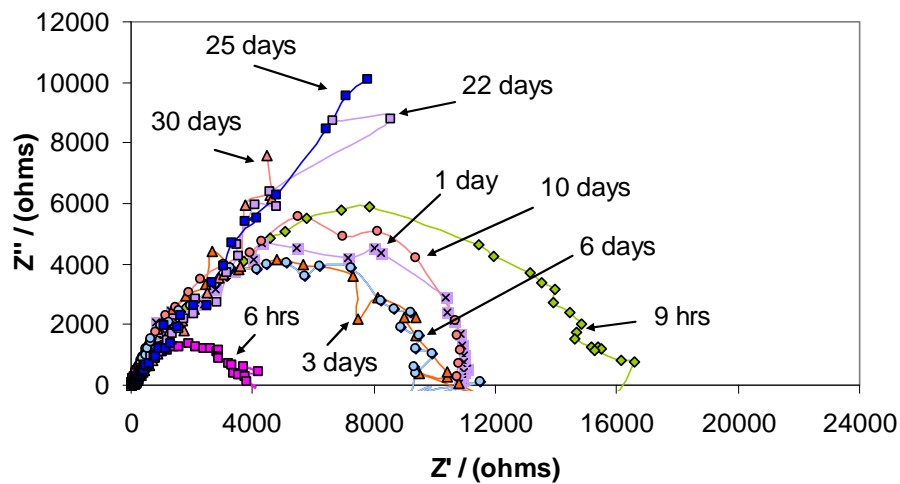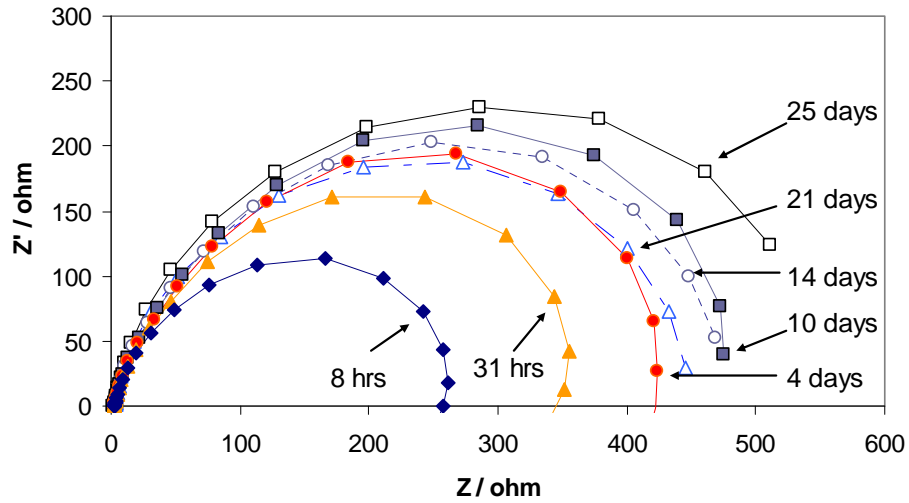

Figure 7. Experiment 2: Change in the shape of Nyquist plot with time from 0 to 30 days. (60°C, 0.77 MPa CO_2, pH 6, $pH_2S = 0.10$ mbar, single phase).

15
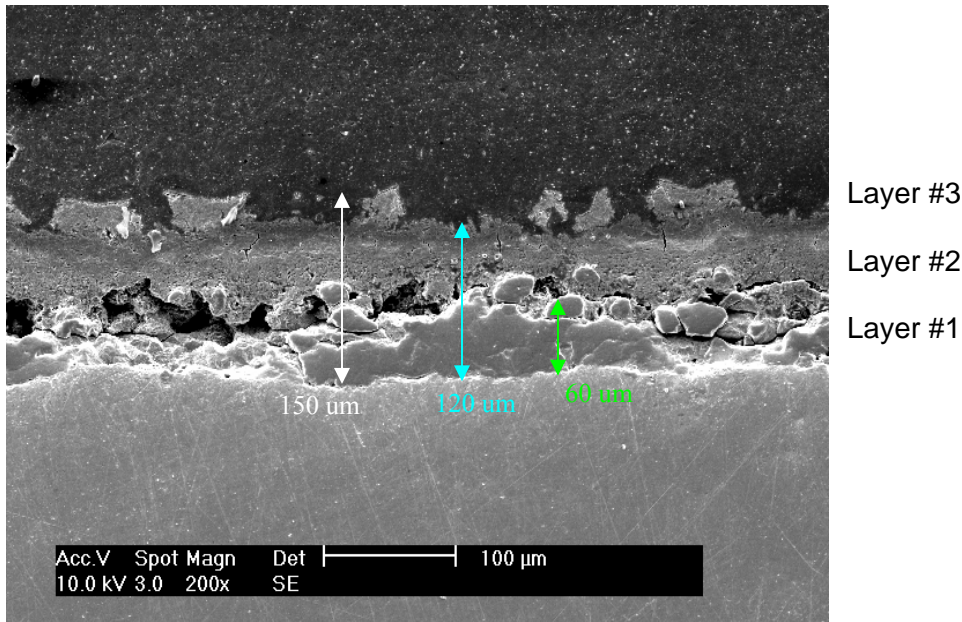
Figure 8. Experiment 3: Cross section of multiphase X65(2) coupon after 25 day exposure(60°C, 0.77 MPa CO_2, pH 6, pH_2S = 1.2 mbar, 25 day exposure). (next to metal surface) layer #1: 60 µm, layer #2: 60 µm, and layer #3: 30 µm. Layer #1 EDS is [32.4% Fe, 0.0% S, 13.4% C, 26.5% O], the interface between layer #1 and layer #2 EDS is [35.4% Fe, 12.9% S, 14.0% C, 9.5% O], and the EDS of layer #2 is [31.2% Fe, 15.0% S, 20.8% C, 11.2% O].

Figure 9. Experiment 3: Change in the shape of the Nyquist plot with time from 8 hours to 25 days. ((60°C, 0.77 MPa CO_2, pH 6, pH_2S = 1.2 mbar, multiphase).
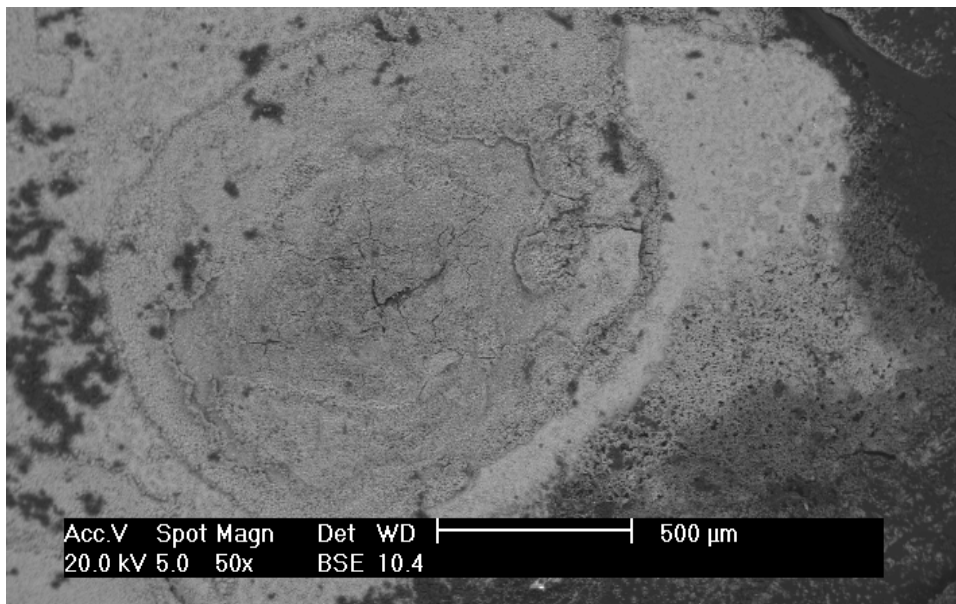
Figure 10. Experiment 4: Surface feature of corrosion product film showing circular pattern observed in many locations. (60°C, P_{total} = 8 bar, pH_2S = 10 mbar [1000ppm], 1 wt% NaCl)
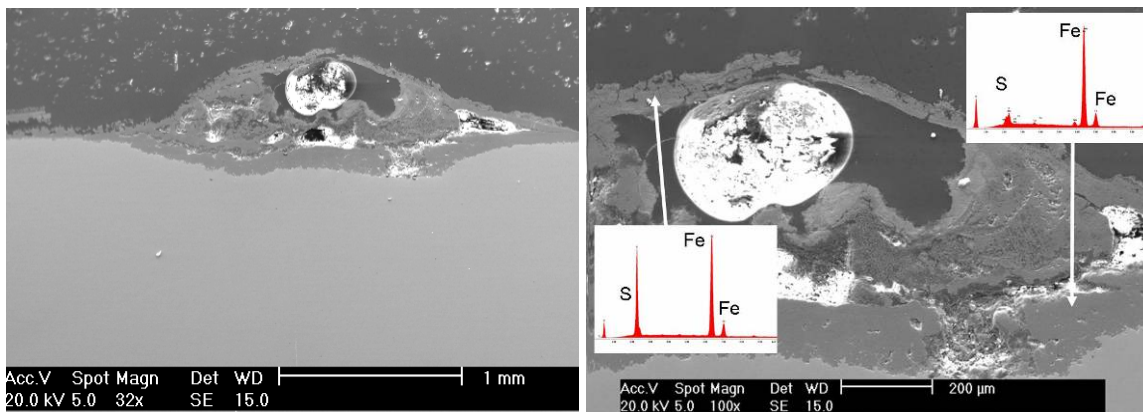

Figure 11. Experiment 4: EDS composition of locations within the localized corrosion. (60°C, P_{total} = 8 bar, pH_2S = 10 mbar [1000ppm], 1 wt% NaCl) The bright circular region in the figure is due to an air bubble captured under the film during epoxy coating of the sample for cross sectioning.
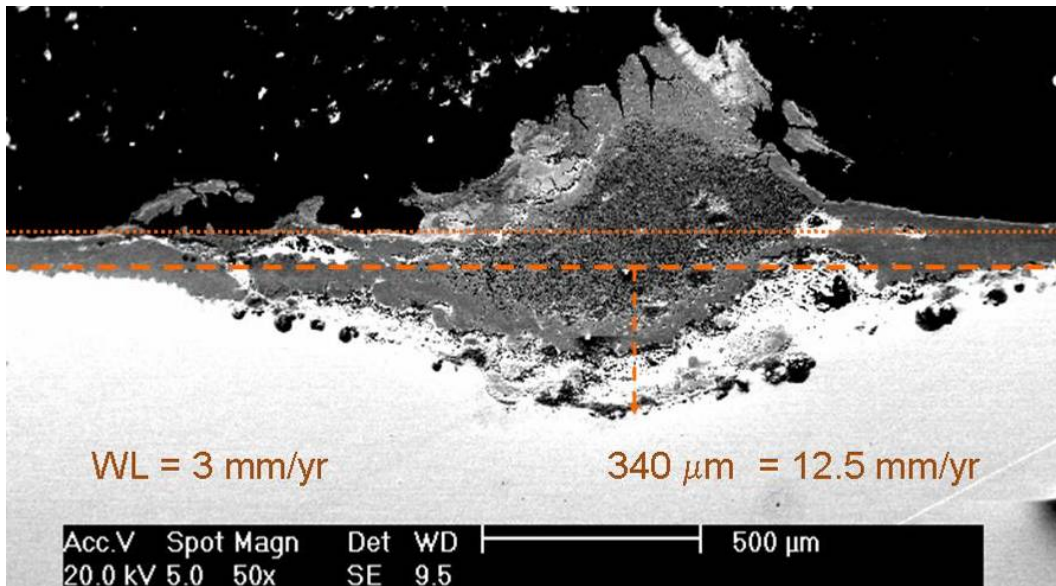
Figure 12. Experiment 4: Cross section - Multiphase flow - 10 days, with calculation of general corrosion rate vs. localized corrosion rate. Pitting Factor: 4.2 (60°C, P_{total} = 8 bar, pH_2S = 10 mbar [1000ppm], 1 wt% NaCl)
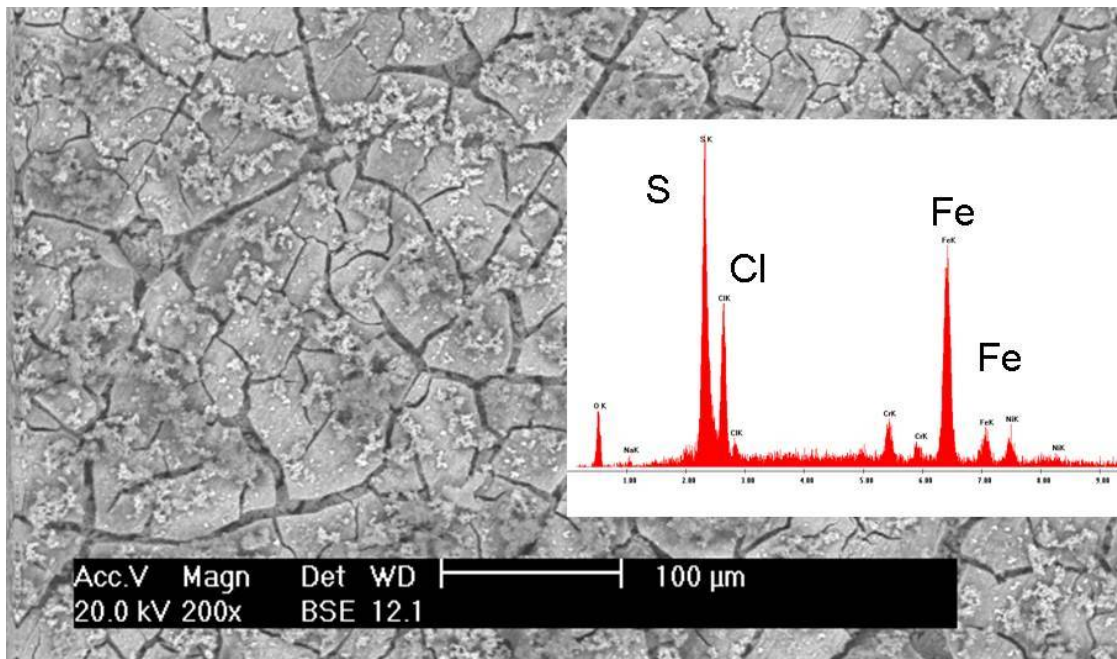

Figure 13. Experiment 5: Surface film from influence of pH_2S and NaCl solution with EDS of film composition. (60°C, P_{total} = 8 bar, pH_2S = 1 mbar [100ppm], 10wt% NaCl).
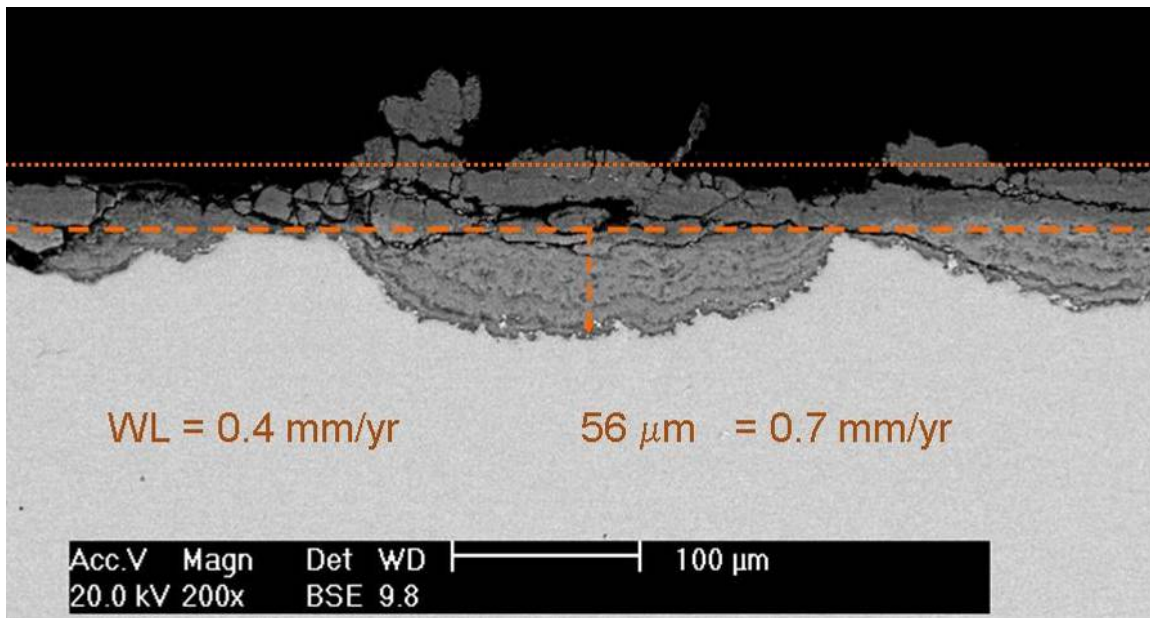
Figure 14. Experiment 5: Cross section of corrosion product film from influence of pH_2S and NaCl solution. (60°C, P_{total} = 8 bar, pH_2S = 1 mbar [100ppm], 10wt% NaCl).
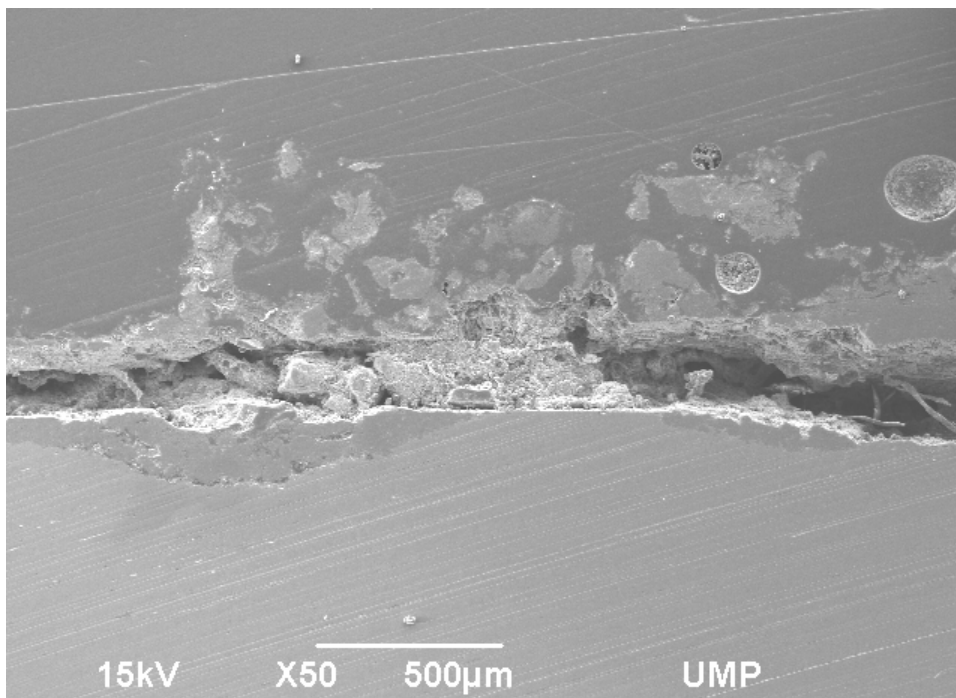

Figure 15. Experiment 6: Cross section of corrosion product film showing 215 μm depth of localized corrosion, 8.0 mm/yr, from the influence of pH_2S and NaCl solution. (60°C, P_{total} = 8 bar, 10 days, Single phase, pCO_2 = 7.7 bar, pH 6.0, 10 mbar H_2S, 10 wt% NaCl)

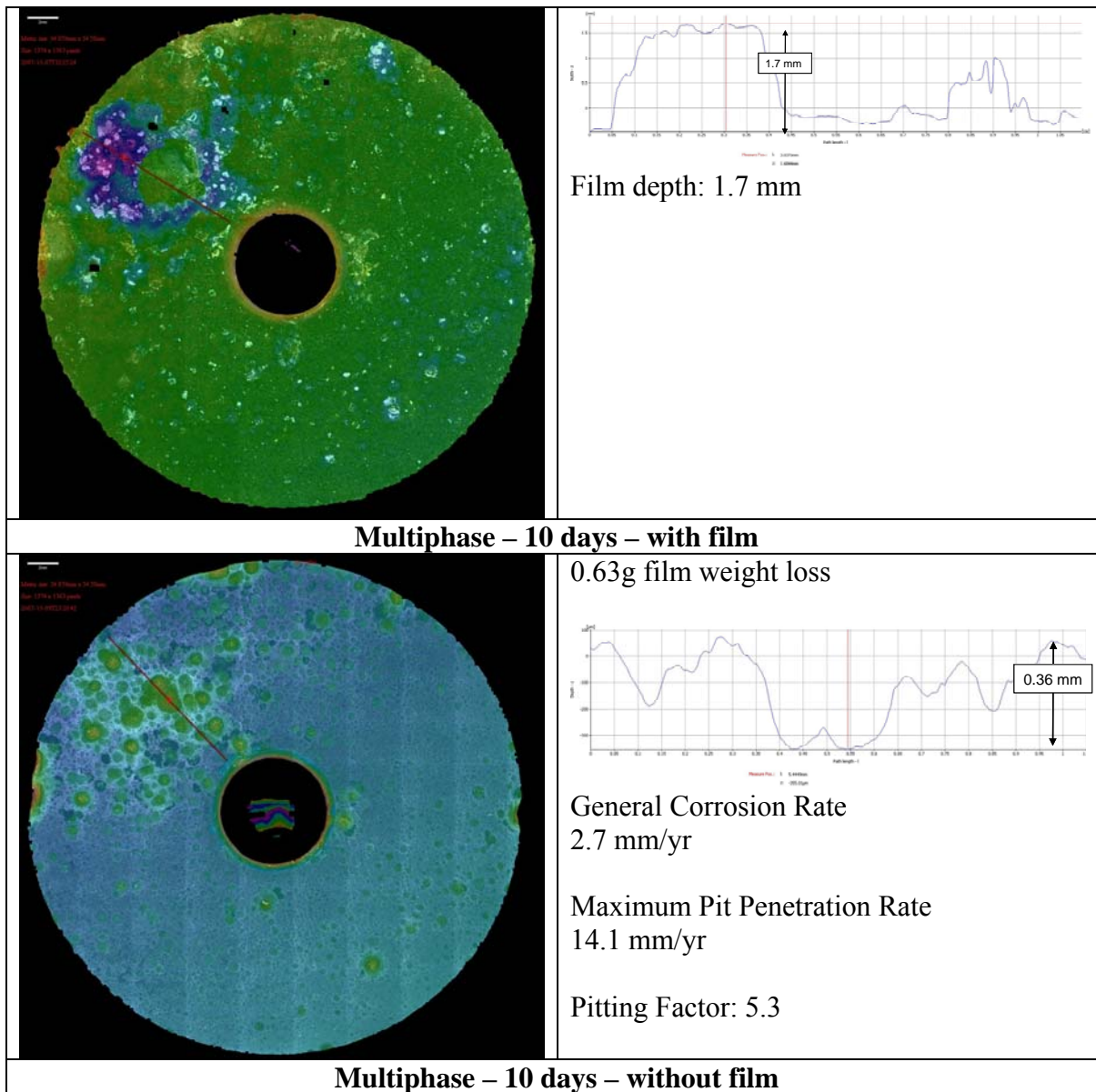| | Film depth: 1.7 mm |

Multiphase – 10 days – with film

| | 0.63g film weight loss |

General Corrosion Rate
2.7 mm/yr

Maximum Pit Penetration Rate
14.1 mm/yr

Pitting Factor: 5.3

Multiphase – 10 days – without film

Figure 16. Experiment 6: Multiphase, 10 days, 60°C, $pCO2$ = 7.7 bar, pH 6.0, 10 mbar H_2S, 10 wt% NaCl

0.09g film weight loss

General Corrosion Rate
0.7 mm/yr

Maximum Pit Penetration Rate
2.9 mm/yr

Pitting Factor: 4.0

Single phase – 20 days – without film

0.08g film weight loss

General Corrosion Rate
0.36 mm/yr

Maximum Pit Penetration Rate
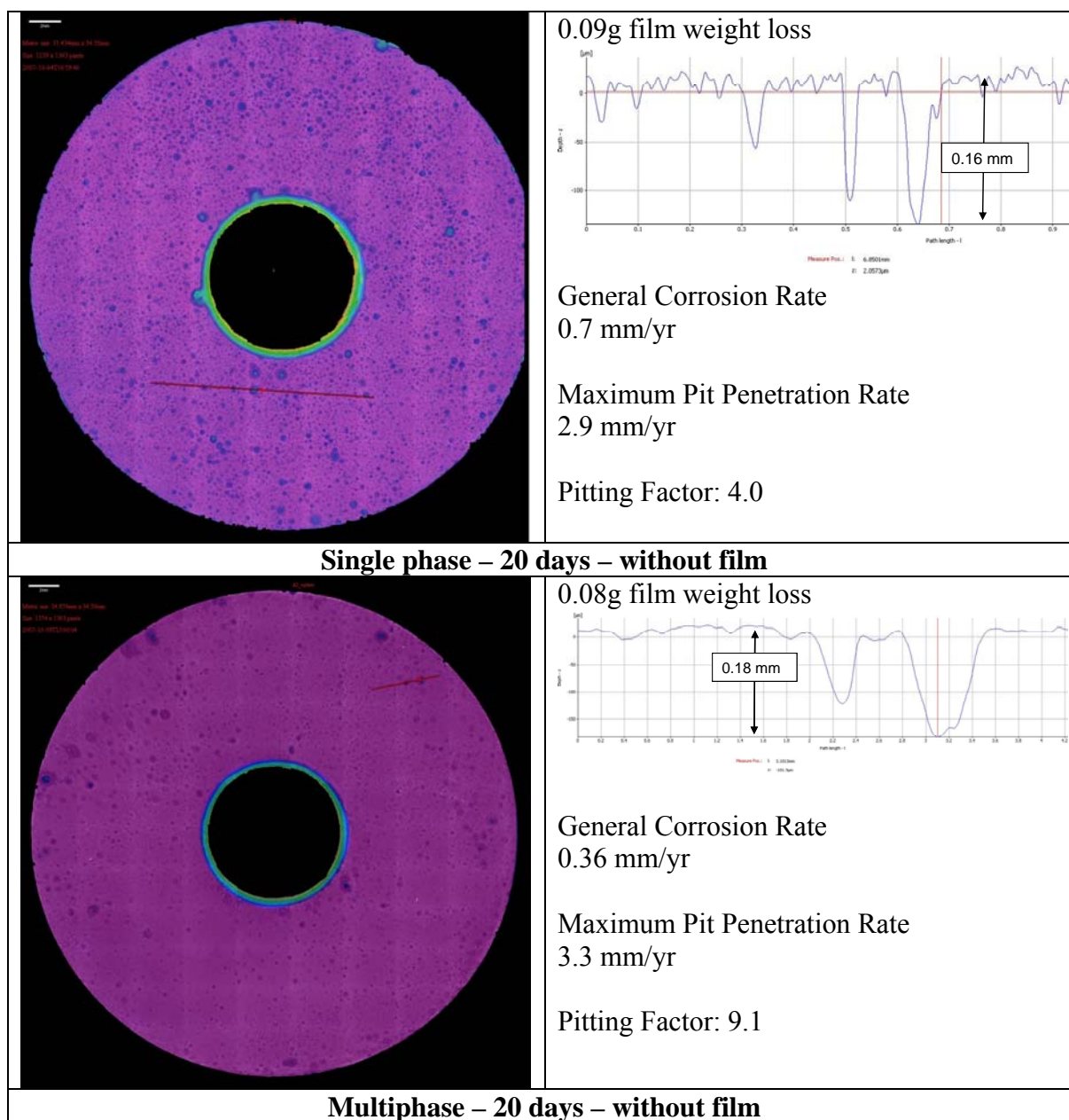3.3 mm/yr

Pitting Factor: 9.1

Multiphase – 20 days – without film

Figure 17. Experiment 6: 20 days exposure to 60°C, $pCO_2 = 7.7$ bar, pH 6.0, 1.0 mbar H_2S, 10 wt% NaCl for single phase and multiphase WL coupons without corrosion product film.
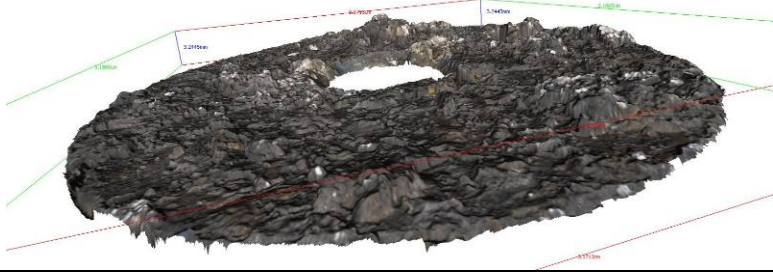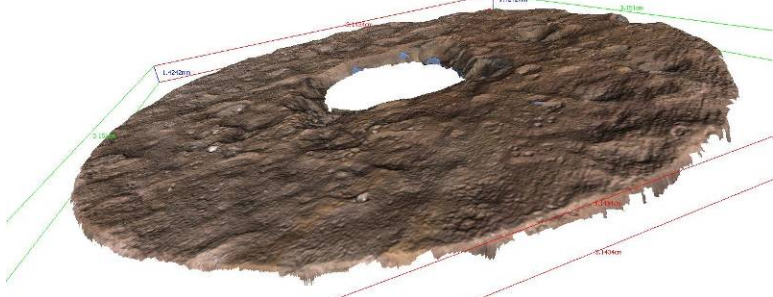
Relationship of Corrosion Product Film to the Corroded Surface	
	(a) Image of corrosion product film developed during 30 day exposure in single phase flow.
	(b) Image of coupon surface after corrosion product film removal by Clark solution. Notice areas of more metal loss occur UNDER peaks of corrosion product film [Image (a)].

Figure 18.   Experiment 6: IFM surface imaging of mild steel coupon exposed for 30 days in single phase flow for conditions 60°C, $pCO_2 = 7.7$ bar, pH 6.0, 10 mbar H_2S, 10 wt% NaCl.

Single phase – 30 days – with film

0.87g film weight loss

General Corrosion Rate
2.5 mm/yr

Maximum Pit Penetration Rate
8.1 mm/yr
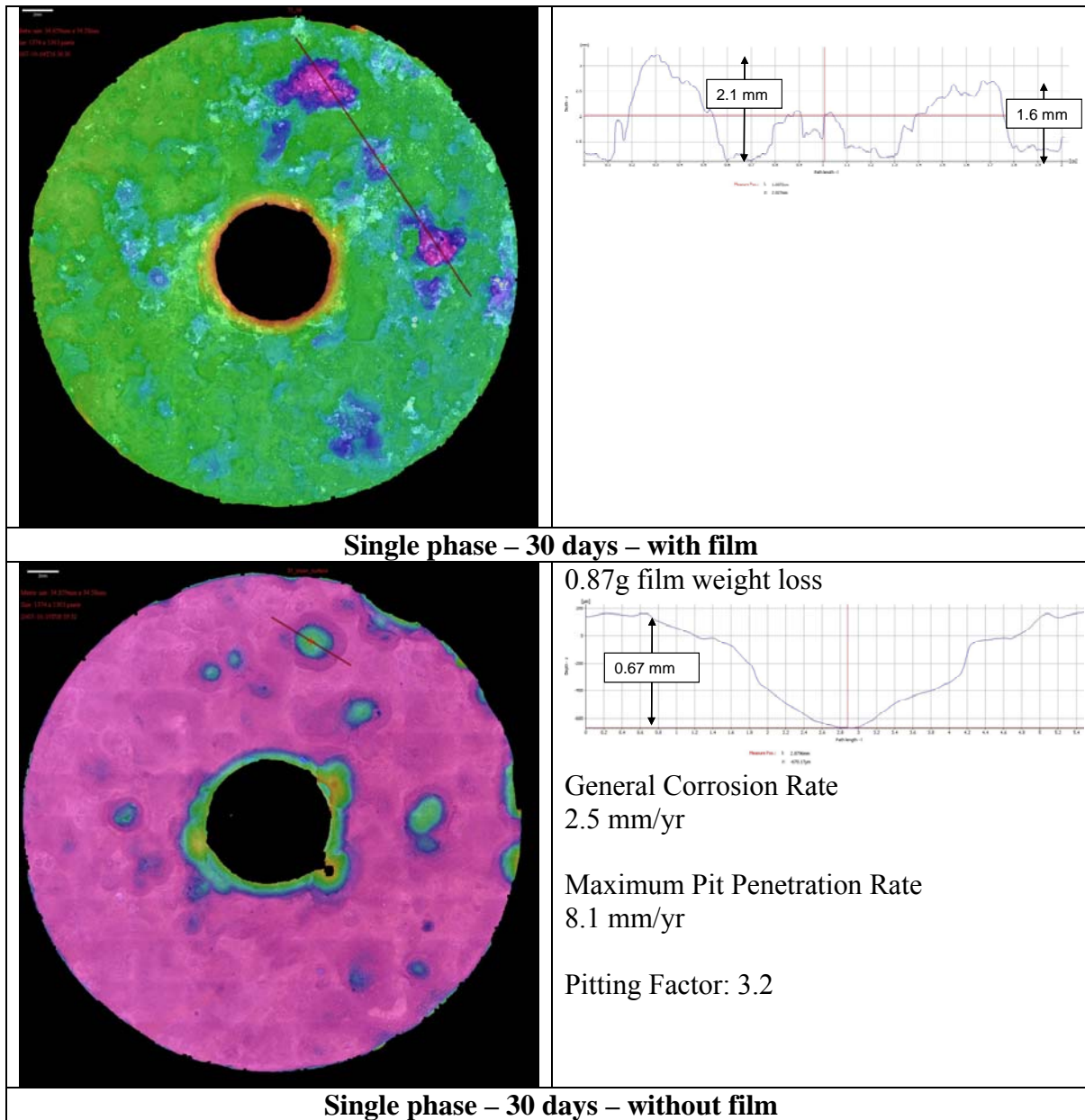
Pitting Factor: 3.2

Single phase – 30 days – without film

Figure 19. Experiment 6: Coupon from single phase flow after 30 days with and without corrosion product film. (60°C, pCO_2 = 7.7 bar, pH 6.0, 10 mbar H_2S, 10 wt% NaCl)

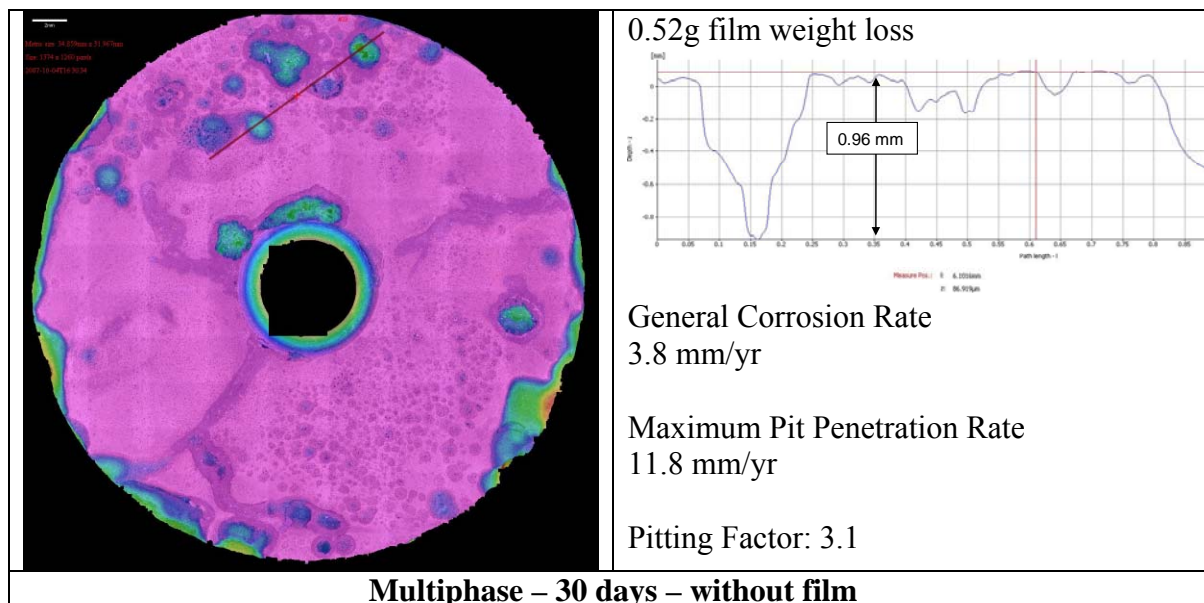|	
	0.52g film weight loss
	General Corrosion Rate 3.8 mm/yr
	Maximum Pit Penetration Rate 11.8 mm/yr
	Pitting Factor: 3.1

Multiphase – 30 days – without film

Figure 20. Experiment 6: IFM surface analysis of mild steel coupon without corrosion product film exposed for 30 days in conditions of 60°C, pCO_2 = 7.7 bar, pH 6.0, 10 mbar H_2S, 10 wt% NaCl